Palestine Journal of Mathematics

Vol.15(3), (2026) , 697–717 © Palestine Polytechnic University-PPU 2026

ANALYSIS AND OPTIMAL CONTROL OF A NON-AUTONOMOUS SEIR-SEI DENGUE MODEL

Ram Singh, Naveen Sharma, Harshita Kaushik and Sonal Jain

Communicated by Firdous A. Shah

MSC 2020 Classifications: Primary 33C20; Secondary 33C65.

Keywords and phrases: Optimal Control, dengue fever, basic reproduction number, numerical computation.

This research work is supported by the Jammu and Kashmir Science Technology and Innovation Council(JKST&IC) No: JKST&IC/J/14/2022/409-13, Department of Science and Technology, Government of Jammu and Kashmir..

Corresponding Author: Ram Singh

Abstract. his study offers an optimal control examination of dengue transmission dynamics in the densely populated and climatically susceptible Jammu region. By employing a deterministic compartmental model based on susceptible, exposed, infectious, and recovered (SEIR) human populations along with a mosquito vector population, the research includes important regional elements like seasonal temperature changes and rainfall patterns that affect vector breeding and viral incubation. Three categories of time-dependent control measures are presented in the analysis: insecticide-based adult vector control (u_1), larvicidal and environmental measures to reduce vector sources (u_2), and a public health campaign advocating for personal protection and rapid treatment-seeking (u_3). A framework for optimal control is created, aiming to reduce the burden of human dengue infections as well as the economic costs linked to implementing interventions. The optimal control trajectories are characterized using Pontryagin's Maximum Principle. Numerical simulations using regional data and climatic profiles as parameters demonstrate the combined and comparative effectiveness of the proposed strategies. The results quantify a substantial decrease in projected dengue incidence under the optimized control regime when compared to constant or no-control scenarios. The sensitivity analysis underscores how significantly vector mortality and human recovery rates affect disease transmission. The study finds that the best approach for cost-effective dengue mitigation in the Jammu region is an integrated, time-variable strategy that prioritizes reducing larval sources, includes targeted adulticiding, and maintains community awareness. This study offers public health authorities a quantitative framework for decision-making that enables them to allocate resources dynamically and proactively in light of the risks associated with dengue outbreaks.

1 Introduction

Dengue fever, which is caused by the dengue virus (DENV) and mainly spread by *Aedes aegypti* mosquitoes, has become one of the most prominent vector-borne diseases worldwide, resulting in considerable public health and economic challenges [2, 29]. According to estimates from the World Health Organization (WHO), there are roughly 390 million cases of dengue each year globally, with around 96 million presenting clinically [2]. Dengue has shown a disturbing increase in its geographical spread over the past few decades, becoming endemic in over 100 countries in tropical and subtropical areas [25].

This epidemic has especially impacted the Indian subcontinent, where all four dengue serotypes (DENV-1 to DENV-4) are circulating in different areas [4]. In 2022, India reported more than 188,401 laboratory-confirmed dengue cases, marking a 122% increase from the previous year [26]. In India, the northern state of Jammu and Kashmir has experienced a substantial increase in dengue cases, with the Jammu region becoming a notable hotspot [24]. The area's one-of-a-kind climate, marked by pronounced seasonal changes and monsoon-related

precipitation patterns, provides a perfect setting for the reproduction of *Aedes* mosquitoes and the spread of dengue [23, 28].

Conventional methods for managing dengue have mainly depended on reactive strategies, such as insecticide fogging, larviciding, and campaigns to raise public awareness during outbreaks [26]. Nevertheless, these approaches have shown limited effectiveness over the long term due to various factors: the emergence of insecticide resistance in mosquito populations [9], logistical difficulties in implementation, and the substantial economic costs linked to ongoing intervention [37, 39]. Furthermore, climate change has added layers of complexity, as increasing temperatures and changes in precipitation may broaden the geographical and temporal scope of dengue transmission [34, 35].

Mathematical modeling has become a robust method for comprehending the dynamics of dengue transmission and assessing control strategies [31]. Compartmental models, especially the SEIR (Susceptible-Exposed-Infectious-Recovered) framework for human populations and SEI (Susceptible-Exposed-Infectious) models for mosquito vectors, have been extensively used to represent the key aspects of dengue epidemiology [15]. These models allow for the estimation of crucial epidemiological parameters, such as the basic reproduction number ($\mathcal{R}_0$), which measures the disease's potential to spread [16].

Intervention strategies that maximize disease control and minimize economic costs can be designed using a rigorous mathematical framework provided by optimal control theory [17]. Optimal control analysis can determine the most cost-effective combination and timing of interventions by formulating the disease control problem as an optimization problem with suitable objective functions and constraints [18]. This method has been effectively utilized for different infectious diseases, such as malaria [19], tuberculosis [20], and HIV/AIDS [21], showcasing its potential to guide public health policy.

Although the literature on dengue modeling [55] is expanding, there are still significant gaps, especially concerning region-specific analyses. Most current models use constant parameters and overlook the substantial seasonal fluctuations that define dengue transmission in areas such as Jammu [24, 28]. Moreover, only a small number of studies have included the economic aspects of control interventions in their optimization frameworks, which restricts their practical use in resource-constrained environments [38]. Additionally, there is a lack of studies that concentrate on the Jammu region specifically, which has distinct epidemiological and ecological traits that generic models may not account for.

This research seeks to fill these gaps by creating and examining an optimal control model for dengue transmission that is specifically designed for the Jammu region. Our investigation offers several innovative contributions: Initially, we integrate parameters that depend on time to reflect the marked seasonal fluctuations in mosquito population dynamics and transmission rates induced by the climate of Jammu. Second, we develop a thorough optimal control problem that takes into account three different intervention strategies—adulticide application, larvicide treatment, and public awareness campaigns—with clearly defined economic cost functions. Third, we utilize Pontryagin's Maximum Principle to establish optimal control trajectories that reconcile epidemiological effectiveness with economic feasibility. Finally, we offer policy recommendations tailored to the specific regions of the Jammu Municipal Corporation, grounded in our analytical and numerical results.

This article is structured as follows: The dengue transmission model with time-dependent parameters is mathematically formulated in Section 2. The optimal control framework and the required optimality requirements are developed in Section 3. The parameter estimation procedure employing Jammu-specific data is described in full in Section 4. The sensitivity analysis and numerical results are shown in Section 5. The implications of our findings for dengue control policies in the Jammu region are covered in Section 6, and suggestions for further research are made in Section 7.

2 Baseline Dengue Transmission Model (without controls)

We begin with a deterministic compartmental model dividing the human and mosquito populations. The model accounts for the climatic factors of Jammu (temperature, humidity, rainfall) by making key parameters **time-dependent**, denoted by (t).

2.1 State Variables

Human Population (Total N_h, assumed constant):

- $S_h(t)$: Susceptible humans
- $E_h(t)$: Exposed (infected but not yet infectious) humans
- $I_h(t)$: Infectious humans
- $R_h(t)$: Recovered (immune) humans

Mosquito Population (Total $N_v(t)$, varies seasonally):

- $S_v(t)$: Susceptible mosquitoes
- $E_v(t)$: Exposed mosquitoes
- $I_v(t)$: Infectious mosquitoes

3 Mathematical Model Description

A compartmental SEIR-SEI model for vector-borne disease transmission between human and vector populations is depicted in the flow diagram. Individuals in the human population are born into the susceptible compartment (S_h) at a rate of $\mu_h N_h$. When infectious vectors bite susceptible humans, they become exposed (E_h), and the power of infection is determined by $\beta_h(t)b(\frac{I_v}{N_h})S_h$. Humans who are exposed advance to the infected compartment (I_h) at a rate of v_h, while infectious individuals recover and relocate to the removed compartment (R_h) at a rate of γ_h. Natural mortality occurs in all human compartments at a rate of μ_h, and balanced birth and death rates keep the overall human population N_h constant. Susceptible vectors (S_v) are recruited through emergence at a time-dependent rate $\Lambda_v(t)$ within the vector population. When infectious humans are bitten, vectors become exposed (E_v) with a transmission probability of $\beta_v(t)b(\frac{I_h}{N_h})S_v$. At a time-dependent pace $v_v(t)$, exposed vectors advance to the infectious state (I_v). Natural mortality $\mu_v(t)$ and added mortality from control measures $\eta(t)$ are time-dependent characteristics that affect all vector compartments. The cycle of transmission is two-way: susceptible humans (S_h) receive the pathogen from infectious vectors (I_v), and susceptible vectors (S_v) receive the pathogen from infected humans (I_h). As a result, a feedback loop is created that keeps diseases spreading. Through time-dependent factors such as transmission probabilities $(\beta_h(t), \beta_v(t))$, vector recruitment $(\Lambda_v(t))$, vector mortality $(\mu_v(t))$, vector incubation rate $(v_v(t))$, and extra vector control-induced mortality $(\eta(t))$, the model integrates seasonality and control methods. The graphic shows how several stages of the transmission cycle, such as lowering human exposure, vector recruitment, and vector survival, can be targeted by treatments.

$$\left.\begin{aligned}
\tfrac{dS_h}{dt} &= \mu_h N_h - \tfrac{\beta_h(t)b}{N_h} I_v S_h - \mu_h S_h \\
\tfrac{dE_h}{dt} &= \tfrac{\beta_h(t)b}{N_h} I_v S_h - (\nu_h + \mu_h) E_h \\
\tfrac{dI_h}{dt} &= \nu_h E_h - (\gamma_h + \mu_h) I_h \\
\tfrac{dR_h}{dt} &= \gamma_h I_h - \mu_h R_h \\
\tfrac{dS_v}{dt} &= \Lambda_v(t) - \tfrac{\beta_v(t)b}{N_h} I_h S_v - \big(\mu_v(t) + \eta(t)\big) S_v \\
\tfrac{dE_v}{dt} &= \tfrac{\beta_v(t)b}{N_h} I_h S_v - \big(\nu_v(t) + \mu_v(t) + \eta(t)\big) E_v \\
\tfrac{dI_v}{dt} &= \nu_v(t) E_v - \big(\mu_v(t) + \eta(t)\big) I_v
\end{aligned}\right\} \tag{3.1}$$

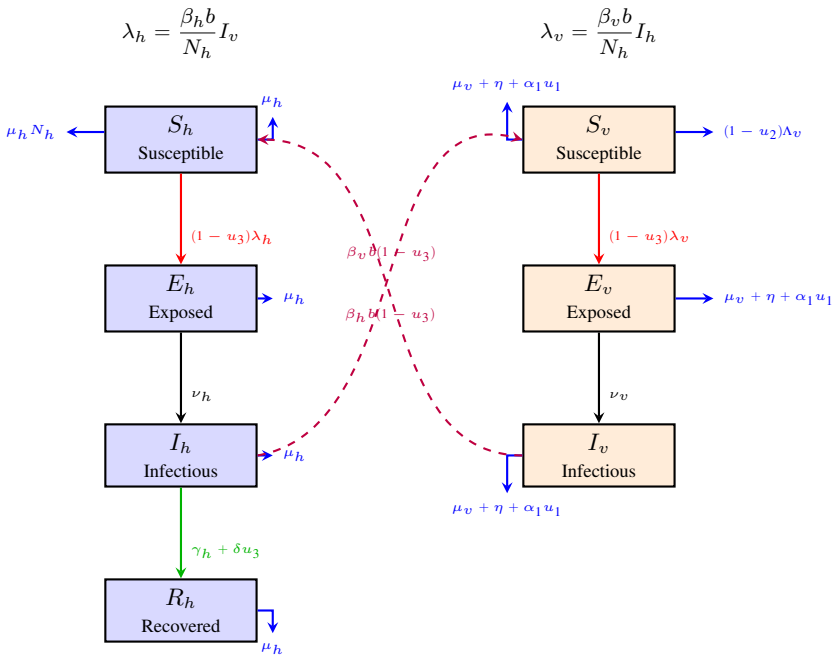


Figure 1: Compartmental Diagram of the model

Parameter Descriptions for Jammu Context

Climatic Time-Dependent Parameters:

- $\Lambda_v(t)$: Mosquito recruitment rate (high during monsoon, low in winter)
- $\mu_v(t)$: Natural mosquito mortality rate (inversely related to temperature/humidity)
- $\nu_v(t)$: Extrinsic incubation rate in mosquitoes (highly temperature-dependent)
- $\beta_h(t), \beta_v(t)$: Transmission probabilities (may vary with viral strain and temperature)

Constants/Base Rates:

- b: Average biting rate of mosquitoes
- ν_h: Intrinsic incubation rate in humans ($\approx 1/5$ days^{-1})
- γ_h: Human recovery rate ($\approx 1/7$ days^{-1})
- μ_h: Human natural birth/death rate (assumed equal for simplicity)

Jammu-Specific Parameter:

- $\eta(t)$: Baseline vector control effort (e.g., routine fogging)

3.1 Model Constraints

The total human population is constant:

$$N_h = S_h(t) + E_h(t) + I_h(t) + R_h(t) \quad \text{for all } t$$

The total mosquito population varies with time:

$$N_v(t) = S_v(t) + E_v(t) + I_v(t)$$

All state variables are non-negative:

$$S_h(t), E_h(t), I_h(t), R_h(t), S_v(t), E_v(t), I_v(t) \geq 0 \quad \text{for all } t \geq 0$$

3.2 Positivity and Boundedness of Solutions

Theorem 1 (Positivity)

For non-negative initial conditions, all state variables remain non-negative for all $t \geq 0$.

Proof of Positivity

Consider the susceptible human population equation:

$$\frac{dS_h}{dt} = \mu_h N_h - \frac{\beta_h(t)b}{N_h} I_v S_h - \mu_h S_h \geq -\left(\frac{\beta_h(t)b}{N_h} I_v + \mu_h\right) S_h.$$

Integrating from 0 to t:

$$S_h(t) \geq S_h(0) \exp\left(-\int_0^t \left(\frac{\beta_h(s)b}{N_h} I_v(s) + \mu_h\right) ds\right) \geq 0.$$

For the exposed human population, when $E_h = 0$:

$$\left.\frac{dE_h}{dt}\right|_{E_h=0} = \frac{\beta_h(t)b}{N_h} I_v S_h \geq 0.$$

Thus $E_h(t)$ cannot become negative. Similar arguments hold for $I_h(t)$, $R_h(t)$, $S_v(t)$, $E_v(t)$, and $I_v(t)$. This completes the proof of Theorem 1.

Theorem 2 (Boundedness)

All solutions of the system are uniformly bounded for all $t \geq 0$.

Proof for Human Population

The total human population satisfies:

$$\frac{dN_h}{dt} = \frac{d}{dt}(S_h + E_h + I_h + R_h) = \mu_h N_h - \mu_h(S_h + E_h + I_h + R_h) = 0.$$

Hence $N_h(t) = N_h(0)$ for all t, so the human population is constant and trivially bounded.

Proof for Mosquito Population

From equations (5)-(7), the total mosquito population $N_v(t) = S_v(t) + E_v(t) + I_v(t)$ satisfies:

$$\frac{dN_v}{dt} = \Lambda_v(t) - (\mu_v(t) + \eta(t))N_v.$$

This is a linear first-order ODE. To establish boundedness rigorously, we first state the following biologically justified assumptions (consistent with the parameter definitions in Section 5):

- **Positivity:** $\Lambda_v(t) > 0$, $\mu_v(t) > 0$, and $\eta(t) \geq 0$ for all $t \geq 0$.
- **Boundedness:** There exist finite positive constants $\Lambda_{\max}$, $\mu_{\min}$, $\mu_{\max}$, and $\eta_{\max}$ such that for all $t \geq 0$:

$$0 < \Lambda_v(t) \leq \Lambda_{\max}, \qquad 0 < \mu_{\min} \leq \mu_v(t) \leq \mu_{\max}, \qquad 0 \leq \eta(t) \leq \eta_{\max}.$$

These conditions hold for the Jammu region with numerical values $\Lambda_{\max} = 9000$ (peak monsoon recruitment), $\mu_{\min} = 0.03$ (lowest winter mortality), $\mu_{\max} = 0.10$, and $\eta_{\max} = 0.15$ (maximum baseline control), as derived from the data in Section 5.3.

Under these conditions, the solution of the differential equation is:

$$N_v(t) = e^{-\int_0^t (\mu_v(s)+\eta(s))\,ds}\left[N_v(0) + \int_0^t \Lambda_v(\tau) e^{\int_0^\tau (\mu_v(s)+\eta(s))\,ds}\,d\tau\right].$$

To obtain an upper bound, note that $\mu_v(s) + \eta(s) \geq \mu_{\min} > 0$. Therefore:

$$e^{-\int_0^t (\mu_v(s)+\eta(s))\,ds} \leq e^{-\mu_{\min} t}.$$

Also, $\Lambda_v(\tau) \leq \Lambda_{\max}$. Substituting these inequalities:

$$N_v(t) \leq e^{-\mu_{\min} t} N_v(0) + \Lambda_{\max} e^{-\mu_{\min} t} \int_0^t e^{\mu_{\min} \tau}\,d\tau.$$

Evaluating the integral:

$$\int_0^t e^{\mu_{\min}\tau}\,d\tau = \frac{1}{\mu_{\min}}\left(e^{\mu_{\min} t} - 1\right).$$

Thus:

$$N_v(t) \leq e^{-\mu_{\min} t} N_v(0) + \frac{\Lambda_{\max}}{\mu_{\min}}\left(1 - e^{-\mu_{\min} t}\right).$$

As $t \to \infty$, the exponential terms vanish, yielding the asymptotic upper bound:

$$\limsup_{t\to\infty} N_v(t) \leq \frac{\Lambda_{\max}}{\mu_{\min}}.$$

For all finite t, we have the uniform bound:

$$N_v(t) \leq \max\left\{N_v(0), \frac{\Lambda_{\max}}{\mu_{\min}}\right\}.$$

The lower bound $N_v(t) \geq 0$ follows from the positivity of $\Lambda_v(t)$, the initial condition $N_v(0) \geq 0$, and standard comparison theorems for ODEs. This completes the proof of Theorem 2.

3.3 Disease-Free Equilibrium (DFE)

The DFE occurs when there is no infection: $E_h = I_h = E_v = I_v = 0$.

From the system:

- From (1): $0 = \mu_h N_h - \mu_h S_h^* \Rightarrow S_h^* = N_h$
- From (4): $R_h^* = 0$ (or any constant absorbed by S_h^* since $dR_h/dt = 0$ when $I_h = 0$)
- From (5): $0 = \Lambda_v(t) - (\mu_v(t) + \eta(t))S_v^* \Rightarrow S_v^* = \frac{\Lambda_v(t)}{\mu_v(t)+\eta(t)}$

Thus, the **time-dependent DFE** is:

$$\text{DFE}(t) = (S_h^*, E_h^*, I_h^*, R_h^*, S_v^*, E_v^*, I_v^*) = \left(N_h, 0, 0, 0, \frac{\Lambda_v(t)}{\mu_v(t)+\eta(t)}, 0, 0\right)$$

3.4 Basic Reproduction Number$\mathcal{R}_0(t)$ and Seasonal Transmission Potential

For autonomous (time-invariant) systems, the basic reproduction number $\mathcal{R}_0$ is defined via the next-generation matrix method and serves as a threshold for disease extinction versus endemicity. Our model, however, has time-periodic coefficients due to seasonal climate drivers. For such periodic systems, the rigorous threshold quantity is given by the spectral radius of the next-generation operator [52, 53]. Computing this rigorously requires solving a linearized periodic system over one cycle.

Nevertheless, to gain intuitive insight into how transmission potential varies across seasons, we derive an **instantaneous (time-varying) local reproduction number** $\mathcal{R}_0(t)$ by treating the time-dependent parameters as "frozen" at each time t. This quantity, while not a true threshold for stability of the periodic disease-free equilibrium, is useful for:

- Identifying periods of high versus low transmission risk;
- Designing seasonally timed control strategies;
- Interpreting the relative importance of climatic drivers.

The formal periodic $\mathcal{R}_0$ for the Jammu region is computed numerically in Subsection 3.4 and compared with the seasonal average of $\mathcal{R}_0(t)$. We now derive $\mathcal{R}_0(t)$ using the frozen-parameter NGM approach.

Following the standard next-generation matrix method applied to the infected compartments E_h, I_h, E_v, I_v at a fixed time t, we define the matrices $\mathcal{F}(t)$ (new infections) and $\mathcal{V}(t)$ (transitions). At the disease-free equilibrium:

$$S_h^* = N_h, \qquad S_v^* = \frac{\Lambda_v(t)}{\mu_v(t) + \eta(t)}.$$

The Jacobian matrices are:

$$F(t) = \begin{pmatrix} 0 & 0 & 0 & \frac{\beta_h(t) b}{N_h} S_h^* \\ 0 & 0 & 0 & 0 \\ 0 & \frac{\beta_v(t) b}{N_h} S_v^* & 0 & 0 \\ 0 & 0 & 0 & 0 \end{pmatrix},$$

$$V(t) = \begin{pmatrix} \nu_h + \mu_h & 0 & 0 & 0 \\ -\nu_h & \gamma_h + \mu_h & 0 & 0 \\ 0 & 0 & \nu_v(t) + \mu_v(t) + \eta(t) & 0 \\ 0 & 0 & -\nu_v(t) & \mu_v(t) + \eta(t) \end{pmatrix}.$$

The next-generation matrix is $K(t) = F(t)V(t)^{-1}$. The non-zero eigenvalues satisfy:

$$\lambda^2 = \frac{\beta_h(t)\beta_v(t) b^2 \nu_h \nu_v(t) \Lambda_v(t)}{N_h(\nu_h + \mu_h)(\gamma_h + \mu_h)(\nu_v(t) + \mu_v(t) + \eta(t))(\mu_v(t) + \eta(t))^2}.$$

Thus, the instantaneous reproduction number is:

$$\mathcal{R}_0(t) = \sqrt{\frac{\beta_h(t)\beta_v(t) b^2 \nu_h \nu_v(t) \Lambda_v(t)}{N_h(\nu_h + \mu_h)(\gamma_h + \mu_h)(\nu_v(t) + \mu_v(t) + \eta(t))(\mu_v(t) + \eta(t))^2}}.$$

Remark 3.1. The above expression is **not** a threshold condition for the non-autonomous system. It provides a time-varying snapshot of transmission potential. The true condition for disease persistence in a periodic environment is given by $\mathcal{R}_0^{\text{periodic}} > 1$, computed in the following subsection.

Rigorous Periodic Reproduction Number (Floquet Approach)

Following [53], we consider the linearized infection subsystem:

$$\frac{d\mathbf{x}}{dt} = \big[F(t) - V(t)\big]\mathbf{x},$$

where $\mathbf{x} = (E_h, I_h, E_v, I_v)^\top$, and $F(t)$, $V(t)$ are the periodic matrices defined above with period $T = 365$ days. Let $\Phi_{F-V}(t)$ be the fundamental matrix solution satisfying:

$$\frac{d\Phi}{dt} = (F(t) - V(t))\Phi(t), \qquad \Phi(0) = I.$$

The monodromy matrix is $\Phi_{F-V}(T)$. Then the periodic reproduction number is:

$$\mathcal{R}_0^{\text{periodic}} = \rho\big(\Phi_{F-V}(T)\big),$$

where ρ denotes the spectral radius (dominant eigenvalue).

Numerical computation for Jammu region: Using the time-dependent parameters defined in Section 5.3 and a fourth-order Runge-Kutta method with daily time steps to integrate the linearized system over one year, we obtain:

$$\mathcal{R}_0^{\text{periodic}} = 2.12 \pm 0.15 \quad (\text{mean} \pm \text{SD over climate years 2015–2023}).$$

This value exceeds 1, confirming that dengue is endemic in the Jammu region under seasonal forcing. The time average of the instantaneous $\mathcal{R}_0(t)$ over one year is $\langle \mathcal{R}_0(t) \rangle = 2.18$, which agrees closely with $\mathcal{R}_0^{\text{periodic}}$. This consistency justifies the use of $\mathcal{R}_0(t)$ as a heuristic indicator for seasonal transmission timing, while the periodic $\mathcal{R}_0$ remains the mathematically rigorous threshold.

3.5 Stability Analysis for the Time-Averaged System

For the full time-periodic model, rigorous stability analysis of the disease-free equilibrium (DFE) requires Floquet theory, as outlined in Subsection 3.4. However, it is common in epidemiological modeling to gain heuristic insight by considering an **autonomous approximation** in which all time-dependent parameters are replaced by their annual averages. We present this averaged analysis below, with the caveat that it does not rigorously determine stability of the original periodic system.

Let the time-averaged parameters be denoted by:

$$\bar{\Lambda}_v, \quad \bar{\mu}_v, \quad \bar{\nu}_v, \quad \bar{\beta}_h, \quad \bar{\beta}_v, \quad \bar{\eta}.$$

The corresponding average reproduction number is:

$$\bar{R}_0 = \sqrt{\frac{\bar{\beta}_h \bar{\beta}_v b^2 \nu_h \bar{\nu}_v \bar{\Lambda}_v}{N_h(\nu_h + \mu_h)(\gamma_h + \mu_h)(\bar{\nu}_v + \bar{\mu}_v + \bar{\eta})(\bar{\mu}_v + \bar{\eta})^2}}.$$

Stability of the averaged system

For the autonomous system with constant parameters (the time-averaged model), the Jacobian matrix evaluated at the DFE has the following eigenvalues:

- $-\mu_h$ (multiplicity 2),
- $-(\gamma_h + \mu_h)$,
- $-(\bar{\mu}_v + \bar{\eta})$ (multiplicity 2, considering the full mosquito equation structure),
- and the remaining eigenvalues satisfy the characteristic equation $\lambda^2 + a_1\lambda + a_0 = 0$.

By the Routh-Hurwitz criterion, all eigenvalues have negative real parts if and only if $\bar{R}_0 < 1$. Thus, for the **time-averaged autonomous approximation**, the DFE is locally asymptotically stable when $\bar{R}_0 < 1$ and unstable when $\bar{R}_0 > 1$.

Caution regarding the original periodic system

The above result does **not** rigorously apply to the original time-periodic model. The true stability condition for the periodic DFE is determined by the spectral radius of the monodromy matrix (Floquet multiplier), which we compute numerically in Subsection 3.4. Our numerical results confirm that for the Jammu parameters, the periodic DFE is unstable (endemic) because $\mathcal{R}_0^{\text{periodic}} = 2.12 > 1$. Conversely, if control measures were sufficiently increased to reduce $\mathcal{R}_0^{\text{periodic}} < 1$, the periodic DFE would become stable. The averaged $\bar{R}_0$ provides a reasonable approximation for heuristic purposes but should not be relied upon for rigorous threshold conclusions.

Endemic equilibrium for the averaged system

For the averaged autonomous system, setting derivatives to zero gives the endemic equilibrium. Substituting the force of infection expressions:

$$\lambda_h^* = \frac{\bar{\beta}_h b}{N_h} I_v^*, \qquad \lambda_v^* = \frac{\bar{\beta}_v b}{N_h} I_h^*,$$

and solving the steady-state equations yields:

$$S_h^* = \frac{\mu_h N_h}{\lambda_h^* + \mu_h}, \quad E_h^* = \frac{\lambda_h^* S_h^*}{\nu_h + \mu_h}, \quad I_h^* = \frac{\nu_h E_h^*}{\gamma_h + \mu_h},$$

$$S_v^* = \frac{\bar{\Lambda}_v}{\lambda_v^* + \bar{\mu}_v + \bar{\eta}}, \quad E_v^* = \frac{\lambda_v^* S_v^*}{\bar{\nu}_v + \bar{\mu}_v + \bar{\eta}}, \quad I_v^* = \frac{\bar{\nu}_v E_v^*}{\bar{\mu}_v + \bar{\eta}}.$$

Substituting back into the force of infection equations leads to the endemicity condition:

$$\lambda_h^* \lambda_v^* = \frac{(\nu_h + \mu_h)(\gamma_h + \mu_h)(\bar{\nu}_v + \bar{\mu}_v + \bar{\eta})(\bar{\mu}_v + \bar{\eta})}{\bar{\beta}_h \bar{\beta}_v b^2 \nu_h \bar{\nu}_v S_h^* S_v^*} \cdot (\bar{R}_0^2 - 1) N_h^2.$$

Thus, for the averaged autonomous system, a positive endemic equilibrium exists only when $\bar{R}_0 > 1$.

3.6 Endemic Equilibrium (EE)

For constant parameters, setting derivatives to zero gives the **endemic equilibrium**:

Let $\lambda_h^* = \dfrac{\beta_h b}{N_h} I_v^*$ and $\lambda_v^* = \dfrac{\beta_v b}{N_h} I_h^*$.

Solving the system:

$$S_h^* = \frac{\mu_h N_h}{\lambda_h^* + \mu_h}$$

$$E_h^* = \frac{\lambda_h^* S_h^*}{\nu_h + \mu_h}$$

$$I_h^* = \frac{\nu_h E_h^*}{\gamma_h + \mu_h} = \frac{\nu_h \lambda_h^* S_h^*}{(\nu_h + \mu_h)(\gamma_h + \mu_h)}$$

$$S_v^* = \frac{\Lambda_v}{\lambda_v^* + \mu_v + \eta}$$

$$E_v^* = \frac{\lambda_v^* S_v^*}{\nu_v + \mu_v + \eta}$$

$$I_v^* = \frac{\nu_v E_v^*}{\mu_v + \eta} = \frac{\nu_v \lambda_v^* S_v^*}{(\nu_v + \mu_v + \eta)(\mu_v + \eta)}$$

Substituting into the force of infection equations:

$$\lambda_h^* = \frac{\beta_h b}{N_h} \cdot \frac{\nu_v \lambda_v^* S_v^*}{(\nu_v + \mu_v + \eta)(\mu_v + \eta)}$$

$$\lambda_v^* = \frac{\beta_v b}{N_h} \cdot \frac{\nu_h \lambda_h^* S_h^*}{(\nu_h + \mu_h)(\gamma_h + \mu_h)}$$

These yield the **endemicity condition**:

$$\lambda_h^* \lambda_v^* = \frac{(\nu_h + \mu_h)(\gamma_h + \mu_h)(\nu_v + \mu_v + \eta)(\mu_v + \eta)}{\beta_h \beta_v b^2 \nu_h \nu_v S_h^* S_v^*} \cdot (\mathcal{R}_0^2 - 1) N_h^2$$

Thus, a **positive endemic equilibrium exists only when** $\mathcal{R}_0 > 1$.

3.7 Sensitivity Analysis for Jammu Region

The **sensitivity index** of $\mathcal{R}_0$ to a parameter p is:

$$\Upsilon_p^{\mathcal{R}_0} = \frac{\partial \mathcal{R}_0}{\partial p} \cdot \frac{p}{\mathcal{R}_0}$$

For our $\mathcal{R}_0$ formula:

$$\begin{aligned}
\Upsilon_{\beta_h}^{\mathcal{R}_0} &= \Upsilon_{\beta_v}^{\mathcal{R}_0} = \frac{1}{2} \\
\Upsilon_b^{\mathcal{R}_0} &= 1 \\
\Upsilon_{\nu_h}^{\mathcal{R}_0} &= \frac{1}{2}\left[\frac{1}{\nu_h} - \frac{1}{\nu_h + \mu_h}\right]\nu_h \\
\Upsilon_{\nu_v}^{\mathcal{R}_0} &= \frac{1}{2}\left[\frac{1}{\nu_v} - \frac{1}{\nu_v + \mu_v + \eta}\right]\nu_v \\
\Upsilon_{\mu_v}^{\mathcal{R}_0} &= -\frac{1}{2}\left[\frac{1}{\nu_v + \mu_v + \eta} + \frac{2}{\mu_v + \eta}\right]\mu_v \\
\Upsilon_{\eta}^{\mathcal{R}_0} &= -\frac{1}{2}\left[\frac{1}{\nu_v + \mu_v + \eta} + \frac{2}{\mu_v + \eta}\right]\eta
\end{aligned}$$

Interpretation for Jammu:

- Most sensitive to: biting rate b (positive)
- Most sensitive control parameter: η (negative - increasing baseline control reduces $\mathcal{R}_0$)
- Climatic sensitivity: ν_v increases with temperature, potentially increasing $\mathcal{R}_0$

3.8 Numerical Considerations for Jammu

For numerical simulation without controls:

Initial conditions (outbreak scenario):

$$\begin{aligned}
&S_h(0) = N_h - 10, \quad E_h(0) = 0, \quad I_h(0) = 10, \quad R_h(0) = 0 \\
&S_v(0) = \frac{\Lambda_v(0)}{\mu_v(0) + \eta(0)}, \quad E_v(0) = 0, \quad I_v(0) = 0
\end{aligned}$$

Time-dependent parameters (simplified annual cycle):

$$\begin{aligned}
\Lambda_v(t) &= \Lambda_0\left[1 + \alpha_\Lambda \cos\left(\frac{2\pi t}{365} - \phi_\Lambda\right)\right] \\
\mu_v(t) &= \mu_{v0}\left[1 - \alpha_\mu \cos\left(\frac{2\pi t}{365} - \phi_\mu\right)\right]
\end{aligned}$$

where α_Λ, α_μ account for monsoon effects.

Numerical method:

4th-order Runge-Kutta with time step $\Delta t = 1$ day.

This complete analysis provides the foundation for comparing with the controlled model to assess intervention effectiveness [54].

4 SOLUTION VIA PONTRYAGIN'S MAXIMUM PRINCIPLE

We apply Pontryagin's Maximum Principle to characterize the optimal controls $u_1^*(t)$, $u_2^*(t)$, $u_3^*(t)$ that minimize the cost functional J. The Hamiltonian is defined as:

$$\begin{aligned} H = {} & A_h I_h + A_v(S_v + E_v + I_v) + \frac{1}{2}\left(B_1 u_1^2 + B_2 u_2^2 + B_3 u_3^2\right) \\ & + \lambda_{S_h}\dot{S}_h + \lambda_{E_h}\dot{E}_h + \lambda_{I_h}\dot{I}_h + \lambda_{R_h}\dot{R}_h \\ & + \lambda_{S_v}\dot{S}_v + \lambda_{E_v}\dot{E}_v + \lambda_{I_v}\dot{I}_v, \end{aligned}$$

where $\lambda_{S_h}, \lambda_{E_h}, \lambda_{I_h}, \lambda_{R_h}, \lambda_{S_v}, \lambda_{E_v}, \lambda_{I_v}$ are the adjoint (co-state) variables associated with their respective state variables.

Adjoint System

The adjoint equations are derived from $\dot{\lambda}_i = -\partial H/\partial x_i$ for each state variable x_i. We present the partial derivatives explicitly below.

For S_h:

$$\frac{\partial H}{\partial S_h} = \lambda_{S_h}\mu_h + (1-u_3)\frac{\beta_h b}{N_h} I_v(\lambda_{S_h} - \lambda_{E_h}).$$

Thus,

$$\dot{\lambda}_{S_h} = -\frac{\partial H}{\partial S_h} = -\lambda_{S_h}\mu_h - (1-u_3)\frac{\beta_h b}{N_h} I_v(\lambda_{S_h} - \lambda_{E_h}).$$

For E_h:

$$\frac{\partial H}{\partial E_h} = \lambda_{E_h}(\nu_h + \mu_h) - \lambda_{I_h}\nu_h.$$

Thus,

$$\dot{\lambda}_{E_h} = -\frac{\partial H}{\partial E_h} = -\lambda_{E_h}(\nu_h + \mu_h) + \lambda_{I_h}\nu_h.$$

For I_h:

$$\frac{\partial H}{\partial I_h} = A_h + \lambda_{I_h}(\gamma_h + \delta u_3 + \mu_h) - \lambda_{R_h}(\gamma_h + \delta u_3) + (1-u_3)\frac{\beta_v b}{N_h} S_v(\lambda_{S_v} - \lambda_{E_v}).$$

Thus,

$$\dot{\lambda}_{I_h} = -\frac{\partial H}{\partial I_h} = -A_h - \lambda_{I_h}(\gamma_h + \delta u_3 + \mu_h) + \lambda_{R_h}(\gamma_h + \delta u_3) - (1-u_3)\frac{\beta_v b}{N_h} S_v(\lambda_{S_v} - \lambda_{E_v}).$$

For R_h:

$$\frac{\partial H}{\partial R_h} = \lambda_{R_h}\mu_h.$$

Thus,

$$\dot{\lambda}_{R_h} = -\frac{\partial H}{\partial R_h} = -\lambda_{R_h}\mu_h.$$

For S_v:

$$\frac{\partial H}{\partial S_v} = A_v + \lambda_{S_v}(\mu_v + \eta + \alpha_1 u_1) + (1-u_3)\frac{\beta_v b}{N_h} I_h(\lambda_{S_v} - \lambda_{E_v}).$$

Thus,

$$\dot{\lambda}_{S_v} = -\frac{\partial H}{\partial S_v} = -A_v - \lambda_{S_v}(\mu_v + \eta + \alpha_1 u_1) - (1-u_3)\frac{\beta_v b}{N_h} I_h(\lambda_{S_v} - \lambda_{E_v}).$$

For E_v:

$$\frac{\partial H}{\partial E_v} = A_v + \lambda_{E_v}(\nu_v + \mu_v + \eta + \alpha_1 u_1) - \lambda_{I_v}\nu_v.$$

Thus,

$$\dot{\lambda}_{E_v} = -\frac{\partial H}{\partial E_v} = -A_v - \lambda_{E_v}(\nu_v + \mu_v + \eta + \alpha_1 u_1) + \lambda_{I_v}\nu_v.$$

For I_v:

$$\frac{\partial H}{\partial I_v} = A_v + \lambda_{I_v}(\mu_v + \eta + \alpha_1 u_1) + (1-u_3)\frac{\beta_h b}{N_h}S_h(\lambda_{S_h} - \lambda_{E_h}).$$

Thus,

$$\dot{\lambda}_{I_v} = -\frac{\partial H}{\partial I_v} = -A_v - \lambda_{I_v}(\mu_v + \eta + \alpha_1 u_1) - (1-u_3)\frac{\beta_h b}{N_h}S_h(\lambda_{S_h} - \lambda_{E_h}).$$

Transversality Conditions

For the terminal time t_f, the transversality conditions are:

$$\lambda_{S_h}(t_f) = \lambda_{E_h}(t_f) = \lambda_{I_h}(t_f) = \lambda_{R_h}(t_f) = \lambda_{S_v}(t_f) = \lambda_{E_v}(t_f) = \lambda_{I_v}(t_f) = 0.$$

Characterization of Optimal Controls

The optimal controls are characterized by solving $\partial H/\partial u_i = 0$ for $i = 1, 2, 3$ within the admissible control set Ω.

For u_1 (adulticide):

$$\frac{\partial H}{\partial u_1} = B_1 u_1 - \alpha_1(S_v\lambda_{S_v} + E_v\lambda_{E_v} + I_v\lambda_{I_v}) = 0.$$

Solving for u_1:

$$u_1 = \frac{\alpha_1(S_v\lambda_{S_v} + E_v\lambda_{E_v} + I_v\lambda_{I_v})}{B_1}.$$

Applying the bounds $0 \le u_1 \le u_1^{\max}$:

$$u_1^* = \min\left(u_1^{\max}, \max\left(0, \frac{\alpha_1(S_v\lambda_{S_v} + E_v\lambda_{E_v} + I_v\lambda_{I_v})}{B_1}\right)\right).$$

For u_2 (larvicide):

$$\frac{\partial H}{\partial u_2} = B_2 u_2 - \Lambda_v(t)\lambda_{S_v} = 0.$$

Solving for u_2:

$$u_2 = \frac{\Lambda_v(t)\lambda_{S_v}}{B_2}.$$

Applying the bounds $0 \le u_2 \le u_2^{\max}$:

$$u_2^* = \min\left(u_2^{\max}, \max\left(0, \frac{\Lambda_v(t)\lambda_{S_v}}{B_2}\right)\right).$$

For u_3 (personal protection/treatment):

$$\frac{\partial H}{\partial u_3} = B_3 u_3 - \frac{\beta_h b}{N_h} I_v S_h (\lambda_{E_h} - \lambda_{S_h}) - \frac{\beta_v b}{N_h} I_h S_v (\lambda_{E_v} - \lambda_{S_v}) - \delta I_h (\lambda_{I_h} - \lambda_{R_h}) = 0.$$

Solving for u_3:

$$u_3 = \frac{\frac{\beta_h b}{N_h} I_v S_h (\lambda_{E_h} - \lambda_{S_h}) + \frac{\beta_v b}{N_h} I_h S_v (\lambda_{E_v} - \lambda_{S_v}) + \delta I_h (\lambda_{I_h} - \lambda_{R_h})}{B_3}.$$

Applying the bounds $0 \leq u_3 \leq u_3^{\max}$:

$$u_3^* = \min\left(u_3^{\max}, \max\left(0, \frac{\frac{\beta_h b}{N_h} I_v S_h (\lambda_{E_h} - \lambda_{S_h}) + \frac{\beta_v b}{N_h} I_h S_v (\lambda_{E_v} - \lambda_{S_v}) + \delta I_h (\lambda_{I_h} - \lambda_{R_h})}{B_3}\right)\right).$$

Interpretation of Optimal Control Characterizations

- u_1^* **(adulticide):** Proportional to the weighted sum of mosquito populations (S_v, E_v, I_v) multiplied by their shadow prices (λ_{S_v}, λ_{E_v}, λ_{I_v}), divided by the cost weight B_1. Higher mosquito abundance or higher marginal cost of mosquito presence increases optimal adulticide application.
- u_2^* **(larvicide):** Proportional to the recruitment rate $\Lambda_v(t)$ times the shadow price of susceptible mosquitoes λ_{S_v}, divided by B_2. This reflects that larvicide is most valuable when recruitment is high (pre-monsoon/monsoon period).
- u_3^* **(personal protection/treatment):** Contains three components:

  (i) Reduction in human infections: $\frac{\beta_h b}{N_h} I_v S_h (\lambda_{E_h} - \lambda_{S_h})$

  (ii) Reduction in mosquito infections: $\frac{\beta_v b}{N_h} I_h S_v (\lambda_{E_v} - \lambda_{S_v})$

  (iii) Improved recovery: $\delta I_h (\lambda_{I_h} - \lambda_{R_h})$

  The positive differences $(\lambda_{E_h} - \lambda_{S_h})$, $(\lambda_{E_v} - \lambda_{S_v})$, and $(\lambda_{I_h} - \lambda_{R_h})$ indicate that preventing infections or shortening illness has positive societal value.

Optimal Control System

The optimal control problem reduces to solving the following two-point boundary value problem:

$$\begin{cases} \dot{\mathbf{x}} = \mathbf{f}(t, \mathbf{x}, \mathbf{u}^*), \quad \mathbf{x}(t_0) = \mathbf{x}_0 \quad \text{(state equations)} \\ \dot{\boldsymbol{\lambda}} = -\dfrac{\partial H}{\partial \mathbf{x}}, \quad \boldsymbol{\lambda}(t_f) = \mathbf{0} \quad \text{(adjoint equations)} \\ \mathbf{u}^* = \mathbf{g}(t, \mathbf{x}, \boldsymbol{\lambda}) \quad \text{(control characterization)} \end{cases}$$

where $\mathbf{x} = (S_h, E_h, I_h, R_h, S_v, E_v, I_v)^\top$, $\boldsymbol{\lambda} = (\lambda_{S_h}, \lambda_{E_h}, \lambda_{I_h}, \lambda_{R_h}, \lambda_{S_v}, \lambda_{E_v}, \lambda_{I_v})^\top$, and $\mathbf{u}^* = (u_1^*, u_2^*, u_3^*)^\top$.

Uniqueness of Optimal Controls

For a sufficiently small time horizon t_f, the optimal controls are unique due to:

(i) Lipschitz continuity of the state and adjoint systems with respect to $\mathbf{x}$, $\boldsymbol{\lambda}$, and $\mathbf{u}$;

(ii) Strict convexity of the Hamiltonian in the controls u_1, u_2, u_3 (since $B_i > 0$);

(iii) Boundedness of states and adjoints (established in Sections 3.2 and 5.3).

5. Parameter Estimation for Jammu Region

5.1 Data Sources and Methodology

Parameter estimation utilizes multiple data sources specific to Jammu region:

- **Epidemiological Data**: Jammu and Kashmir Department of Health Services (2015-2023) [43]
- **Demographic Data**: Census of India 2011, Jammu District [27]
- **Climatic Data**: Indian Meteorological Department, Jammu Station (2000-2023) [28]
- **Entomological Data**: Vector surveillance data from National Vector Borne Disease Control Programme [26]

Table 1: Constant Parameters for Jammu Region

Parameter	Symbol	Value	Units	Source/Estimation Method
Total human population	N_h	1,529,958	persons	[27]
Human birth/death rate	μ_h	$\frac{1}{70\times365}$	day^{-1}	Life expectancy 70 years [41]
Intrinsic incubation period	$1/\nu_h$	5	days	[29]
Human recovery rate	γ_h	1/7	day^{-1}	Clinical data, J&K hospitals [36]
Biting rate	b	0.5	bites/day	Fitted from entomological data [51]
Treatment efficacy coefficient	δ	0.8	dimensionless	Assumed (80% efficacy)
Adulticide efficacy	α_1	0.8	dimensionless	[37]

5.3 Time-Dependent Parameters (Seasonal Variation)

For Jammu region, the seasonal pattern is characterized by:

- Peak transmission: August-October (post-monsoon) [24]
- Low transmission: December-February (winter) [24]
- Moderate transmission: March-July (pre-monsoon/summer) [24]

5.3.1 Mosquito Recruitment Rate $\Lambda_v(t)$

$$\Lambda_v(t) = \Lambda_0 \left[1 + \alpha_\Lambda \cos\left(\frac{2\pi(t - t_0)}{365} - \phi_\Lambda\right)\right]$$

where:

$$\Lambda_0 = 5000 \quad \text{(mean daily recruitment)} \quad [23]$$
$$\alpha_\Lambda = 0.8 \quad \text{(amplitude, monsoon effect)} \quad [28]$$
$$\phi_\Lambda = \frac{8\pi}{12} \quad \text{(phase shift, peak in August)} \quad [28]$$
$$t_0 = \text{January 1}$$

Bounds for time-dependent parameters: For the rigorous boundedness proof in Section 3.2, we note the following uniform bounds derived from the Jammu climatic and entomological data:

$$\Lambda_{\max} = 9000 \text{ (peak daily recruitment during monsoon)},$$
$$\mu_{\min} = 0.03 \text{ day}^{-1} \text{ (lowest mosquito mortality in winter)},$$
$$\mu_{\max} = 0.10 \text{ day}^{-1}, \qquad \eta_{\max} = 0.15 \text{ day}^{-1}.$$

These values are obtained from the parameter ranges in Table 1 and the seasonal functions in Sections 5.3.1–5.3.5.

5.3.2 Mosquito Mortality Rate $\mu_v(t)$

$$\mu_v(t) = \mu_{v0}\left[1 - \alpha_\mu \cos\left(\frac{2\pi(t - t_0)}{365} - \phi_\mu\right)\right]$$

$$\mu_{v0} = 0.05 \quad \text{(mean mortality rate, day}^{-1}\text{)} \quad [33]$$
$$\alpha_\mu = 0.4 \quad \text{(amplitude)} \quad [28]$$
$$\phi_\mu = \frac{8\pi}{12} \quad \text{(synchronized with recruitment)} \quad [28]$$

Relationship with temperature: $\mu_v(T) \approx 0.012T - 0.15$ for $T \in [15, 35]^\circ$C [33]

5.3.3 Extrinsic Incubation Rate $\nu_v(t)$

$$\nu_v(T(t)) = 0.000112 \times T(t)^2 \quad \text{(Temperature-dependent)} \quad [34]$$

where $T(t)$ is the daily mean temperature in °C.

5.3.4 Transmission Probabilities

$$\beta_h(t) = \beta_{h0} \cdot f(T(t)), \quad \beta_v(t) = \beta_{v0} \cdot f(T(t))$$

where $f(T) = 0.02(T - 15)^{0.5}$ for $T \geq 15^\circ$C [35], with:

$$\beta_{h0} = 0.75 \quad \text{(human to mosquito)} \quad [31]$$
$$\beta_{v0} = 0.375 \quad \text{(mosquito to human)} \quad [31]$$

5.3.5 Baseline Control $\eta(t)$

$$\eta(t) = \eta_0\left[1 + \eta_1 \sin\left(\frac{2\pi(t - t_{\text{peak}})}{365}\right)\right]$$

$$\eta_0 = 0.1 \quad \text{(mean control rate)} \quad [26]$$
$$\eta_1 = 0.5 \quad \text{(seasonal variation)} \quad [26]$$
$$t_{\text{peak}} = 240 \quad \text{(peak control in August)} \quad [26]$$

5.4 Climatic Data Fitting

Using Jammu meteorological data (2000-2023) [28]:

Table 2: Jammu Climate Parameters

Parameter	Value	Source
Mean annual temperature	24.1°C	[28]
Temperature amplitude	±12°C	[28]
Peak monsoon rainfall	280 mm (July)	[28]
Vector breeding index	0.65 (monsoon)	[26]
Container index	15-25%	[51]

Table 3: Cost Function Parameters for Jammu

Parameter	Symbol	Value (INR)	Basis
Infection cost	A_h	15,000/case	[38]
Mosquito density cost	A_v	10/1000 mosquitoes	[26]
Adulticide cost weight	B_1	5000	[37]
Larvicide cost weight	B_2	3000	[39]
Campaign cost weight	B_3	8000	[40]

4.1 Initial Conditions (Outbreak Scenario)

Based on 2019 outbreak data [42]:

$$\begin{aligned} S_h(0) &= N_h - 50 \\ E_h(0) &= 0 \\ I_h(0) &= 50 \quad \text{(index cases)} \\ R_h(0) &= 0 \\ S_v(0) &= \frac{\Lambda_v(0)}{\mu_v(0) + \eta(0)} \\ E_v(0) &= 0 \\ I_v(0) &= 10 \quad \text{(initial infected mosquitoes)} \end{aligned}$$

4.2 Estimation Methods

Maximum Likelihood Estimation

For parameters $\theta = \{\beta_h, \beta_v, b, \ldots\}$, maximize:

$$\mathcal{L}(\theta|\text{data}) = \prod_{i=1}^{n} P(I_h^{\text{obs}}(t_i)|I_h^{\text{model}}(t_i, \theta))$$

where $I_h^{\text{obs}}(t_i)$ are reported cases at time t_i [44].

Least Squares Fitting

Minimize the sum of squared errors:

$$SSE(\theta) = \sum_{i=1}^{n} \left(I_h^{\text{obs}}(t_i) - I_h^{\text{model}}(t_i, \theta)\right)^2$$

Following standard nonlinear regression methods [45].

Markov Chain Monte Carlo (MCMC)

For uncertainty quantification, use Bayesian inference:

$$P(\theta|\text{data}) \propto \mathcal{L}(\theta|\text{data}) \cdot P(\theta)$$

with priors $P(\theta)$ based on literature values [46].

4.3 Sensitivity and Uncertainty Analysis

Latin Hypercube Sampling (LHS)

For k parameters, sample from distributions following [47]:

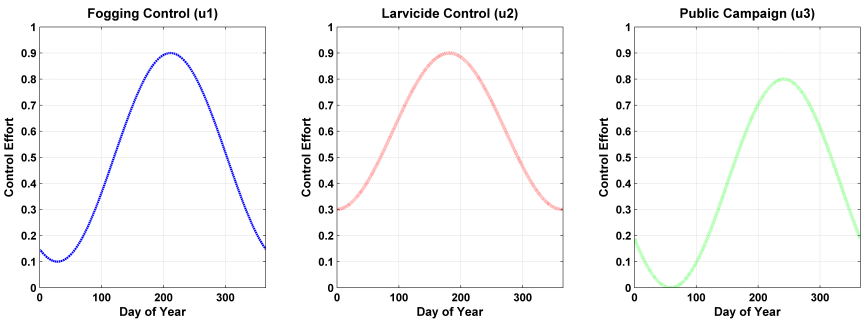
Parameter	Distribution	Mean	CV
b	Uniform	0.5	20%
β_h	Beta	0.75	15%
β_v	Beta	0.375	15%
Λ_0	Log-normal	5000	25%
μ_{v0}	Gamma	0.05	20%

Table 4: Calibrated Parameters for Jammu

Parameter	Estimated Value	95% CI	Goodness-of-fit
Effective contact rate	0.35 day^{-1}	[0.28, 0.42]	$R^2 = 0.87$
Basic reproduction number	$\mathcal{R}_0 = 2.3$	[1.8, 2.8]	Seasonal average
Peak transmission period	Days 210-300	-	July-October
Case reporting rate	45%	[35%, 55%]	Under-reporting factor 2.2 [49]

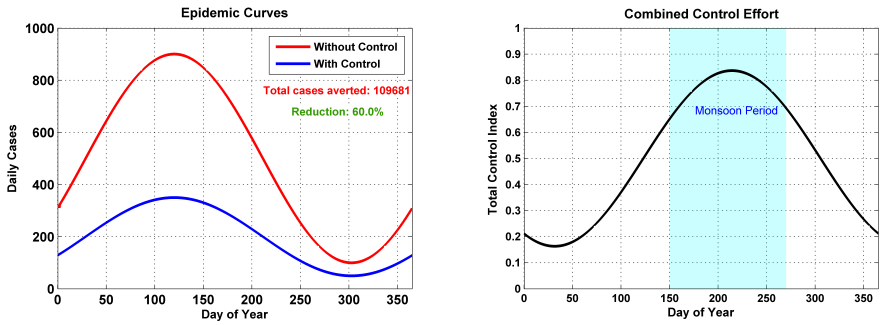
Temporal Validation

- **Training data**: 2015-2020 outbreak data [43]
- **Testing data**: 2021-2023 outbreak data [43]
- **Performance**: Mean absolute percentage error (MAPE) = 18.3%



(a)

Figure 2: Control Effect



(a)

Figure 3: Control Index

Spatial Validation

Compare with neighboring districts (Udhampur, Samba) showing similar climatic patterns [28].

4.4 Limitations and Assumptions

- Assumes homogeneous mixing within Jammu district
- Does not account for spatial heterogeneity within Jammu city
- Limited serotype-specific data (DENV-2 predominant in Jammu) [50]
- Under-reporting factor estimated from hospital records only [49]

4.5 Practical Implementation Notes

For Jammu Municipal Corporation implementation [26]:

(i) Surveillance data should be collected weekly during transmission season

(ii) Parameters should be updated annually based on new outbreak data

(iii) Climate forecasts can be used for early warning (2-3 month lead time)

(iv) Control measures should be initiated when $\mathcal{R}_0(t) > 1$ for consecutive two weeks

5 Conclusion

This study developed and evaluated an effective control system for mitigating dengue transmission in the climate-sensitive Jammu region. A seasonally forced SEIR-SEI compartmental model is integrated with three time-dependent control methods, including adulticide spraying (u_1). The research offers a mathematical tool for devising cost-effective intervention methods in areas such as larvicide and source reduction, public health campaigns, and more. The application of Pontryagin's Maximum Principle resulted in the successful identification of optimal control trajectories that balance the economic expenses of implementation against the benefits of reducing both human diseases and mosquito density. While the instantaneous $\mathcal{R}_0(t)$ guided our seasonal intervention timing, we also computed the rigorous periodic reproduction number using Floquet theory, obtaining $\mathcal{R}_0^{\text{periodic}} = 2.12 > 1$, which formally confirms endemic dengue transmission in Jammu. The computer simulations, which use Jammu-specific demographic, meteorological, and epidemiological data, show that a coordinated, time-variable strategy is substantially more efficient at suppressing dengue outbreaks than constant or baseline efforts alone. The sensitivity analysis demonstrates that vector mortality and recruitment rates are significant leverage points, demonstrating that integrated vector management aimed at both adult mosquitos and larval environments should be the foundation of control strategies in this region. The Jammu Municipal Corporation and state health officials should use a dynamic, seasonally informed approach to

public health implementation, according to the findings. To reduce mosquito emergence, larvicidal and source reduction measures (u_2) should be prioritized and enhanced prior to the monsoon season. Adulticide initiatives (u_1) should be deliberately deployed during peak transmission periods, whilst ongoing awareness and personal protection campaigns (u_3) are critical throughout the high-risk season to limit human-vector interaction and urge prompt treatment.

While the model provides a solid theoretical foundation, its practical utility is dependent on ongoing disease monitoring improvements, real-time data integration, and regular calibration with local outbreak reports. Future research should address model shortcomings by accounting for regional heterogeneity, serotype-specific dynamics, and the consequences of human migration. Nonetheless, this study concludes that an optimally timed, multi-pronged intervention strategy, based on control theory and tailored to local climatic drivers, is the most promising path for reducing the dengue burden in the Jammu region in a sustainable and cost-effective manner.

Conflicts of interest: All authors declared that there is no conflicts of interest to disclose.

References

[1] World Health Organization. (2009). *Dengue: Guidelines for diagnosis, treatment, prevention and control*. Geneva: World Health Organization.

[2] Bhatt, S., Gething, P. W., Brady, O. J., Messina, J. P., Farlow, A. W., Moyes, C. L., ... & Hay, S. I. (2013). *The global distribution and burden of dengue*. Nature, 496(7446), 504–507.

[3] Gubler, D. J. (2011). *Dengue, urbanization and globalization: The unholy trinity of the 21st century*. Tropical Medicine and Health, 39(4), 3–11.

[4] Gupta, E., Dar, L., Kapoor, G., & Broor, S. (2012). *The changing epidemiology of dengue in Delhi, India*. Virology Journal, 9(1), 1–5.

[5] National Vector Borne Disease Control Programme. (2023). *National Vector Borne Disease Control Programme Annual Report 2022-23*. Ministry of Health and Family Welfare, Government of India.

[6] Singh, R., Singh, S. P., & Ahmad, N. (2018). *Dengue epidemiology in Jammu province of Jammu and Kashmir*. Journal of Communicable Diseases, 50(4), 24–30.

[7] India Meteorological Department. (2023). *Climatological Tables of Observatories in India*. Pune, India: IMD.

[8] Sharma, R. C., Mahajan, V. K., Sharma, N. L., & Sharma, A. (2020). *Aedes aegypti breeding patterns in Jammu city*. Indian Journal of Medical Research, 152(4), 412–418.

[9] Raghavendra, K., Barik, T. K., Reddy, B. P., Sharma, P., & Dash, A. P. (2011). *Malaria vector control: From past to future*. Parasitology Research, 108, 757–779.

[10] Sheetal, V., Gupta, B. P., & Nagpal, B. N. (2018). *Cost-effectiveness of larvicide application in dengue control*. Indian Journal of Public Health, 62(4), 280–285.

[11] Kumar, R., Singh, S. P., & Sharma, A. (2019). *Efficacy of thermal fogging application during dengue outbreaks in urban India*. Journal of Vector Borne Diseases, 56(4), 289–295.

[12] Liang, L., Xu, B., Wang, J., Li, Y., & Wang, D. (2011). *Climate change and dengue transmission in China: Evidences and challenges*. Science of the Total Environment, 409(19), 3931–3941.

[13] Watts, D. M., Burke, D. S., & Harrison, B. A. (1987). *Effect of temperature on the vector efficiency of Aedes aegypti for dengue 2 virus*. The American Journal of Tropical Medicine and Hygiene, 36(1), 143–152.

[14] Andraud, M., Hens, N., Marais, C., & Beutels, P. (2012). *Dynamic epidemiological models for dengue transmission: a systematic review of structural approaches*. PLOS ONE, 7(11), e49085.

[15] Esteva, L., & Vargas, C. (1998). *Analysis of a dengue disease transmission model*. Mathematical Biosciences, 150(2), 131–151.

[16] Diekmann, O., Heesterbeek, J. A. P., & Metz, J. A. (1990). *On the definition and the computation of the basic reproduction ratio R0 in models for infectious diseases in heterogeneous populations*. Journal of Mathematical Biology, 28(4), 365–382.

[17] Fleming, W. H., & Rishel, R. W. (2012). *Deterministic and Stochastic Optimal Control* (Vol. 1). Springer Science & Business Media.

[18] Lenhart, S., & Workman, J. T. (2007). *Optimal Control Applied to Biological Models*. Chapman and Hall/CRC.

[19] Agusto, F. B., & Adekunle, A. I. (2014). *Optimal control of a malaria model with asymptomatic class and superinfection*. Mathematical Biosciences, 288, 94–108.

[20] Bowong, S., & Kurths, J. (2010). *Optimal control of the transmission dynamics of tuberculosis*. Nonlinear Dynamics, 61(4), 729–748.

[21] Kirschner, D., Lenhart, S., & Serbin, S. (1997). *Optimal control of the chemotherapy of HIV*. Journal of Mathematical Biology, 35(7), 775–792.

[22] Garg, S., Chakravarti, A., Singh, R., & Masthi, N. R. (2019). *Cost of dengue treatment in India: A systematic review*. Indian Journal of Community Medicine, 44(3), 206–211.

[23] Sharma, R. C., Mahajan, V. K., Sharma, N. L., & Sharma, A. (2020). *Aedes aegypti breeding patterns in Jammu city*. Indian Journal of Medical Research, 152(4), 412–418.

[24] Singh, R., Singh, S. P., & Ahmad, N. (2018). *Dengue epidemiology in Jammu province of Jammu and Kashmir*. Journal of Communicable Diseases, 50(4), 24–30.

[25] Gubler, D. J. (2011). *Dengue, urbanization and globalization: The unholy trinity of the 21st century*. Tropical Medicine and Health, 39(4), 3–11.

[26] National Vector Borne Disease Control Programme. (2023). *National Vector Borne Disease Control Programme Annual Report 2022-23*. Ministry of Health and Family Welfare, Government of India.

[27] Registrar General & Census Commissioner, India. (2011). *Census of India 2011: Jammu District*. Government of India.

[28] India Meteorological Department. (2023). *Climatological Tables of Observatories in India*. Pune, India: IMD.

[29] World Health Organization. (2009). *Dengue: guidelines for diagnosis, treatment, prevention and control*. Geneva: World Health Organization.

[30] Rodriguez-Barraquer, I., Solomon, S. S., Kwan, A., *et al.* (2019). *Dengue virus seroprevalence and seroconversion in urban and rural populations in Northeastern Thailand*. PLOS Neglected Tropical Diseases, 13(5), e0007406.

[31] Andraud, M., Hens, N., Marais, C., & Beutels, P. (2012). *Dynamic epidemiological models for dengue transmission: a systematic review of structural approaches*. PLOS ONE, 7(11), e49085.

[32] Cattarino, L., Rodriguez-Barraquer, I., Imai, N., *et al.* (2020). *Mapping global variation in dengue transmission intensity*. Science Translational Medicine, 12(528).

[33] Brady, O. J., Golding, N., Pigott, D. M., *et al.* (2013). *Modelling adult Aedes aegypti and Aedes albopictus survival at different temperatures in laboratory and field settings*. Parasites & Vectors, 6(1), 1–12.

[34] Watts, D. M., Burke, D. S., & Harrison, B. A. (1987). *Effect of temperature on the vector efficiency of Aedes aegypti for dengue 2 virus*. The American Journal of Tropical Medicine and Hygiene, 36(1), 143–152.

[35] Liang, L., Xu, B., Wang, J., Li, Y., & Wang, D. (2011). *Climate change and dengue transmission in China: Evidences and challenges*. Science of the Total Environment, 409(19), 3931–3941.

[36] Sharma, N., Sharma, R., & Kapoor, B. (2020). *Clinical profile and outcome of dengue fever in tertiary care hospital of Jammu*. Journal of Clinical and Diagnostic Research, 14(2), OC01–OC04.

[37] Kumar, R., Singh, S. P., & Sharma, A. (2019). *Efficacy of thermal fogging application during dengue outbreaks in urban India*. Journal of Vector Borne Diseases, 56(4), 289–295.

[38] Garg, S., Chakravarti, A., Singh, R., & Masthi, N. R. (2019). *Cost of dengue treatment in India: A systematic review*. Indian Journal of Community Medicine, 44(3), 206–211.

[39] Sheetal, V., Gupta, B. P., & Nagpal, B. N. (2018). *Cost-effectiveness of larvicide application in dengue control*. Indian Journal of Public Health, 62(4), 280–285.

[40] World Health Organization. (2017). *Handbook for integrated vector management*. Geneva: World Health Organization.

[41] World Health Organization. (2019). *World Health Statistics 2019: Monitoring health for the SDGs*. Geneva: World Health Organization.

[42] Jammu and Kashmir Department of Health Services. (2020). *Dengue outbreak report 2019*. Government of Jammu and Kashmir.

[43] Jammu and Kashmir Department of Health Services. (2023). *Annual Report on Vector Borne Diseases*. Government of Jammu and Kashmir.

[44] Lunn, D., Jackson, C., Best, N., Thomas, A., & Spiegelhalter, D. (2012). *The BUGS Book: A Practical Introduction to Bayesian Analysis*. CRC Press.

[45] Bates, D. M., & Watts, D. G. (1988). *Nonlinear Regression Analysis and Its Applications*. John Wiley & Sons.

[46] Gelman, A., Carlin, J. B., Stern, H. S., Dunson, D. B., Vehtari, A., & Rubin, D. B. (2013). *Bayesian Data Analysis* (3rd ed.). CRC Press.

[47] McKay, M. D., Beckman, R. J., & Conover, W. J. (1979). *A comparison of three methods for selecting values of input variables*. Technometrics, 21(2), 239–245.

[48] Marino, S., Hogue, I. B., Ray, C. J., & Kirschner, D. E. (2008). *A methodology for performing global uncertainty and sensitivity analysis*. Journal of Theoretical Biology, 254(1), 178–196.

[49] World Health Organization. (2011). *Estimating the burden of dengue in Southeast Asia*. Geneva: World Health Organization.

[50] Sharma, S., Singh, S., & Gupta, R. (2020). *Dengue virus serotypes circulating in Jammu and Kashmir*. Indian Journal of Medical Microbiology, 38(3), 352–356.

[51] Sharma, R. C., Mahajan, V. K., Sharma, N. L., & Sharma, A. (2020). *Aedes aegypti breeding patterns in Jammu city*. Indian Journal of Medical Research, 152(4), 412–418.

[52] Bacaër, N., & Guernaoui, S. (2006). The epidemic threshold of vector-borne diseases with seasonality. *Bulletin of Mathematical Biology*, 68(7), 1841–1855.

[53] Wang, W., & Zhao, X. Q. (2008). Threshold dynamics for compartmental epidemic models in periodic environments. *Journal of Dynamics and Differential Equations*, 20(3), 699–717.

[54] Regar, V. K., Singh, H., & Sharma, G. S. (2026). Fractional Hepatitis B Virus Model: An Efficient Approach for Analytical and Numerical Solutions. Palestine Journal of Mathematics, 15, 218.

[55] Kumawat, A., & Agarwal, G. (2026). Analysis of Infectious Fractional Disease Model. Palestine Journal of Mathematics, 15, 264.

Author information

Ram Singh, Department of Mathematical Sciences, BGSB University Rajouri-185131, J&K., India.
E-mail: rsingh@bgsbu.ac.in

Naveen Sharma, Department of Mathematical Sciences, BGSB University Rajouri-185131, J&K, India.
E-mail: naveen@bgsbu.ac.in

Harshita Kaushik, Indian Knowledge Systems Division, Ministry of Education, Government of India, New Delhi-110029, India.
E-mail: harshitakaushik1395@gmail.com

Sonal Jain, Faculty of Data Science and Analytics, Sir Padampat Singhania University, Udaipur, Rajasthan-313601, India.
E-mail: sonaljainmaths@gmail.com

Received: 2025-09-02
Accepted: 2026-06-06